Probing the Lithium–Sulfur Redox Reactions: A Rotating-Ring Disk Electrode Study

ARTICLE *in* THE JOURNAL OF PHYSICAL CHEMISTRY C · MARCH 2014

Impact Factor: 4.77 · DOI: 10.1021/jp500382s

THE JOURNAL OF PHYSICAL CHEMISTRY C

Article

pubs.acs.org/JPCC

Probing the Lithium−Sulfur Redox Reactions: A Rotating-Ring Disk Electrode Study

Yi-Chun Lu,*[,†,‡] Qi He,[†] and Hubert A. Gasteiger[†]

[†]Chair of Technical Electrochemistry, Technische Universität München, Lichtenbergstrasse 4, 22 D-85748, Garching, Germany

[‡]Department of Mechanical and Automation Engineering, The Chinese University of Hong Kong, Shatin N.T., Hong Kong SAR, China

Supporting Information

ABSTRACT: Detailed mechanistic understanding of sulfur redox reactions is critical for developing efficient and stable lithium−sulfur batteries. Here, we employ the rotating-ring disk electrode technique to probe the reaction kinetics and reaction mechanism of lithium−sulfur redox reactions in dimethyl sulfoxide and 1,3-dioxolane:1,2-dimethoxyethane. We quantitatively determine the number of electrons involved in the reduction reactions and the specific activity of sulfur reduction reactions. We show that the electrochemical steps of sulfur reduction exhibit fast reaction kinetics and only account for approximately one-quarter of the total capacity (i.e., ≈4 e^-/S_8) within the short reaction time in RRDE experiments (seconds). The complete conversion of sulfur to Li_2S can only be accomplished via chemical (i.e., potential-independent) polysulfide recombination/dissociation reactions that generate electrochemically reducible polysulfides with long reaction time (hours) in a closed battery cell. The influence of the solvent's solvation power on the rate capability of the sulfur reduction/oxidation processes and the implications for lithium−sulfur batteries will be discussed.

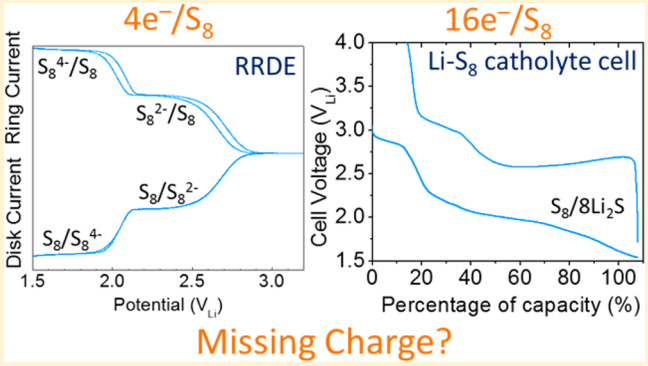

INTRODUCTION

Rechargeable lithium−sulfur (Li−S) batteries promise to provide a 2 to 3 times higher specific energy than conventional Li ion batteries.[1−3] The development of Li−S batteries is strongly hindered by poor rechargeability, limited rate capability, rapid capacity fading, and a poorly controlled/understood electrode−electrolyte interface.[1−4] Detailed mechanistic understanding of Li−S redox reactions is critical for realizing efficient and long-lasting rechargeable Li−S batteries.

Fundamental studies on the electrochemical reduction and oxidation of elemental sulfur on flat model electrodes (e.g., glassy carbon (GC), gold, platinum) in nonaqueous media have been extensively investigated in the past, mostly using high-dielectric solvents like acetonitrile (ACN),[5] dimethyl formamide (DMF),[6−10] and dimethyl sulfoxide (DMSO);[11−15] to our knowledge, only two such studies (flat model electrodes) were conducted with low-dieletric solvents like 1,2-dimethoxyethane (DME) and diglyme[16] or ionic liquids.[17] Using cyclic voltammetry (CV) coupled with spectro-electrochemistry and short-term potential-controlled electrolysis as well as rotating disk electrode (RDE) and microelectrode techniques, it is generally agreed now that the first step in the reduction of sulfur in high-dielectric solvents is[5,8,9,11,13−15]

$$S_8 + 2\,e^- \rightarrow S_8^{2-} \quad (1)$$

This initial electrochemical reduction step is followed by subsequent disproportionation reactions:[5,11,14,15]

$$S_8^{2-} \leftrightarrow S_6^{2-} + (1/4)S_8 \quad (2)$$

$$S_6^{2-} \leftrightarrow 2S_3^{\bullet -} \quad (3)$$

whereby the formation of the blue $S_3^{\bullet -}$ radicals (absorption at ca. 610 nm) in high-dielectric solvents was verified by electron spin resonance measurements;[14,15,18,19] its formation is favored in high-dielectric solvents.[19,20] During longer-term electrolysis at a potential where reaction 1 occurs, additional reducible S_8 is produced by reaction 2, so that the observed reduction charge increases from 2 e^-/S_8 to 8/3 e^-/S_8 (i.e., summing up reactions 1 and 2: $(3/4)S_8 + 2\,e^- \rightarrow S_6^{2-}$).[5,14] At more negative potentials, i.e., in the second reduction wave observed in cyclic voltammograms, another 2-electron reduction step occurs:

$$S_8^{2-} + 2\,e^- \rightarrow S_8^{4-} \rightarrow 2S_4^{2-} \quad (4)$$

whereby the formation of S_4^{2-} has been confirmed by UV/vis spectroscopy.[5,12,14,15] While reaction 4 is commonly agreed upon, it is only opposed by Levillain and co-workers,[8,21,22] who examined the redox behaviors of chemically made Li_2S_6

Received: January 13, 2014
Revised: February 20, 2014
Published: February 24, 2014

   dx.doi.org/10.1021/jp500382s | J. Phys. Chem. C 2014, 118, 5733−5741

solution and proposed that S_6^{2-} and S_8^{2-} cannot be reduced directly and that only the radical anions $S_4^{\bullet-}$ and $S_3^{\bullet-}$ formed by dissociation of S_8^{2-} and S_6^{2-}, respectively, can be further reduced ($S_4^{\bullet-} + e^- \rightarrow S_4^{2-}$ and $S_3^{\bullet-} + e^- \rightarrow S_3^{2-}$). The above reaction steps have been deduced from measurements in high-dielectric solvents in which polysulfide dianions and radicals are highly stable. Jung et al.[16] examined the solvent's influence on the Li−S redox reactions on flat model electrodes and showed that in low-dielectric solvents (DME, diglyme) the two above-described reduction steps are much less separated in potential compared to high-dielectric solvents (DMF, DMSO) and that the first oxidation wave (i.e., previously assigned to $S_8^{4-} \rightarrow S_8^{2-} + 2e^-$)[15] nearly disappears in low-dielectric solvents. The authors thus conclude that the solvent's ability to solvate the primary polysulfide reduction products will influence the reduction/oxidation processes.[16]

In all of the above studies, the maximum reduction charge obtained is ≈4 e^-/S_8 for potentials as low as +1 to +1.5 V vs Li/Li^+, i.e., significantly lower than the 12 to 16 e^-/S_8 which are obtained for long-term discharge curves (fraction of hours to hours) in battery cells using electrodes based on high-surface-area carbons.[1−4,23,24] This suggests that the complete reduction of sulfur to Li_2S (corresponding to 16 e^-/S_8) requires the occurrence of presumably slower chemical reactions between the observed polysulfide intermediates (S_6^{2-} and S_4^{2-}) in the above-described short-term (seconds to minutes) sulfur reduction experiments by means of polysulfide recombination/dissociation solution-phase reactions, examples of which are

$$2S_4^{2-} \leftrightarrow S_7^{2-} + S_1^{2-} \leftrightarrow S_6^{2-} + S_2^{2-} \leftrightarrow S_5^{2-} + S_3^{2-} \quad (5)$$

$$2S_6^{2-} \leftrightarrow S_8^{2-} + S_4^{2-} \leftrightarrow S_7^{2-} + S_5^{2-} \quad (6)$$

While it is in principle possible that S_6^{2-} and S_4^{2-} could be further reduced electrochemically, as was proposed by Barchasz et al.,[25] this is very unlikely since no such reduction steps were ever observed in any of the above-described cyclic voltammetric studies for potentials as low as +1 V vs Li/Li^+. Quite clearly, due to the complex nature of sulfur redox reactions, i.e., the many possible electrochemical steps and chemical reactions, further studies are needed to reveal the sulfur reduction reaction mechanism in lithium−sulfur batteries. This is furthermore complicated by the fact that discharge reaction studies (i.e., sulfur reduction) in battery cell tests have been conducted primarily with low-dielectric solvents (e.g., tetraglyme,[4,25−28] mixtures of 1,3-dioxolane (DOL)[27] and DME,[4,27−29] and ionic liquids[30,31]) in which the reactivity of polysulfide intermediates may be very different from those in high-dielectric solvents (e.g., high abundance of $S_3^{\bullet-}$ radicals in high-dielectric solvents in contrast to low-dielectric solvents).[19,20]

To close this gap, we will examine the differences in sulfur charge/discharge behavior in low- vs high-dielectric solvents and over short and long time scales using rotating-ring disk voltammetry (RRDE) and galvanostatic characterization in a battery cell, respectively. Rotating-ring disk electrode (RRDE) voltammetry has been widely applied to study the reaction kinetics and transport properties of the oxygen reduction reaction (ORR) relevant to metal−air[32,33] batteries. In this report, we exploit RRDE to investigate the reaction mechanism of S reduction/oxidation in a commonly used low-dielectric electrolyte solvent for rechargeable Li−S batteries, namely, DOL:DME (1:1 v:v) and a well-studied high-dielectric solvent, DMSO. We quantitatively determine the number of electrons involved in the reduction reactions and the specific activity of S reduction in DMSO and DOL:DME. We show that the electrochemical steps of S reduction exhibit fast reaction kinetics and only account for approximately one-quarter of the total capacity (i.e, ≈4 e^-/S_8) within the short reaction time in RRDE experiments (seconds). The complete reduction of sulfur to Li_2S (16 e^-/S_8) can only be accomplished by substantially extending the reaction time (fractions of an hour to hours). We demonstrate this point by using a specially designed battery cell in which polysulfide/sulfur diffusion to the lithium anode is prevented by a lithium ion conducting solid electrolyte. The use of the solid electrolyte eliminates the polysulfide shuttle effect.[34] Note that sulfur is supplied only in its dissolved form to provide 100% sulfur accessibility. This supports the hypothesis that the complete conversion of sulfur to Li_2S can only be accomplished via chemical (i.e., potential-independent) polysulfide recombination/dissociation reactions that generate electrochemically reducible polysulfides. The influence of the solvent's solvation power (related to the dielectric constant) on the rate capability of the sulfur reduction/oxidation processes and the implications for Li−S batteries will be discussed.

■ EXPERIMENTAL SECTION

Anhydrous DMSO (Sigma Aldrich, 99.7%), DOL (Sigma Aldrich, 99.8%), and DME (Sigma Aldrich, 99.9%) were dried over Sylobead MS 564C zeolites (3 Å, Grace Division) for a minimum of 24 h. Lithium perchlorate ($LiClO_4$) (battery grade, 99.99%) and lithium bis(trifluoromethane)sulfonimide (LiTFSI) were dried overnight under dynamic vacuum in a glass oven (Büchi, Flawil, Switzerland) at 110 °C. Elemental sulfur (Sigma Aldrich, 99.98%) was dried under ambient conditions at 75 °C for overnight.

RRDE Measurement. The nonaqueous RRDE configuration used in this study was adopted from that reported by Herranz et al.[32] and detailed in the Supporting Information. Briefly, the working electrode consisted of a PTFE embedded glassy carbon disk of 5.0 mm in diameter surrounded by a gold ring with an internal diameter of 6.5 mm and an external diameter of 7.5 mm (Pine Research Instrumentation, Durham, NC). The reference electrode was assembled in the glovebox at least 30 min before putting together the rest of the electrochemical cell; once ready, it was partially immersed into a beaker containing the electrolyte of interest, along with a piece of Li foil (99.9%, Chemetall, Frankfurt, Germany) connected to a Ni wire (99.98%, Advent). The potential difference between both electrodes was subsequently measured for a minimum of 60 min. 4 mM S_8 was dissolved in pure DMSO and DOL:DME and stirred overnight. The RRDE working electrode, the Pt wire counter electrode, the reference electrode, and a glass bubbler allowing for direct flow of gas into the solution or blanketing atop the electrolyte were all assembled inside the glovebox. Prior to the RRDE measurements, ac impedance measurements to determine the ohmic drop between working and reference electrodes were recorded via applying a 10 mV voltage perturbation (1 MHz to 100 mHz) at open circuit. In the resulting Nyquist plots, the high-frequency intersection with the real axis was taken as the uncompensated solution resistance; the values obtained for 0.2 M $LiClO_4$ in DMSO and 1.0 M LiTFSI in DOL:DME were 185 and 67 Ω, respectively.

dx.doi.org/10.1021/jp500382s | J. Phys. Chem. C 2014, 118, 5733−5741

Li−S Catholyte Cell Assembling. Li−S cells were assembled in an Ar-filled glovebox in the following order: (1) placing a lithium foil onto the stainless steel current collector of the cell, (2) adding 20 μL of electrolyte without S_8 (0.2 M $LiClO_4$ in DMSO/1.0 M LiTFSI in DOL:DME), (3) placing one piece of glass fiber separator (Whatman) 21 mm diameter onto the lithium foil, (4) placing one piece of lithium ion conducting glass ceramic (LICGC),[35] and (5) placing one piece of carbon paper (Toray Paper TGPH030 15 mm diameter, 7.5 mg) and adding 20 μL of 4 mM S_8−0.2 M $LiClO_4$ DMSO or 4 mM S_8−1.0 M LiTFSI DOL:DME. Detailed cell schematics are available elsewhere.[35]

Measurements of Diffusion Coefficient of Polysulfide. Diffusion coefficient of S_8, S_8^{2-}, and S_8^{4-}/S_4^{2-} (denoted as "S_8^{4-}") in DMSO and DOL:DME are determined using a method established previously for oxygen and oxygen radicals.[32] Briefly, the diffusion coefficients of S_8 and polysulfides are determined by fitting a relation between the inverse of the rotation speed and the transient time in potential-stepping experiments, which are detailed in the Supporting Information.

Measurements of Solvent Viscosity. The dynamic viscosity (ν) was measured with controlled shear rate (CSR) test mode with parallel-plate measuring system, using a rotational rheometer (MCR 302, Anton Paar, Graz, Austria). An electrolyte sample was prepared in an Ar-filled glovebox and was filled in the measurement gap between the two parallel plates (PP50) with a diameter of 5 cm and a gap dimension of 0.25 mm (outside of glovebox). The sample was measured three times, using CSR test mode with a shear rate (γ) range from 0.1 s^{-1} to 1000 s^{-1} under controlled 25 °C. The viscosities were taken at shear rate γ = 100 s^{-1}.

RESULTS AND DISCUSSION

Since the electrolyte solvent is known to change the discharge/charge voltages of Li−S cells by tens of millivolts to hundreds of millivolts,[28,36] we first examine the sulfur reduction/oxidation by CV on a stagnant GC electrode in DMSO and DOL:DME based electrolytes. The CVs for the two solvents referenced to a conventional Ag/Ag^+ reference electrode (denoted as V_{Ag}) are shown in Figure 1a.

Solvent's Influence on Sulfur Redox Potentials. In DMSO, the first reduction wave starts at ≈ −0.9 V_{Ag}, followed by the second reduction wave at ≈−1.5 V_{Ag}, which have been attributed to reactions 1 and 4, respectively. While the S_8^{4-} anion is believed to be unstable and to dissociate into $2S_4^{2-}$, this dissociation reaction is slow compared to the time scale of the CV as evidenced by the similar oxidation wave currents for S_8^{4-} which commences at ≈−1.7 V_{Ag} at the positive-going scan.[15] Accordingly, the first and second oxidation waves have been attributed to $S_8^{4-} \rightarrow S_8^{2-} + 2\ e^-$ and $S_8^{2-} \rightarrow S_8 + 2\ e^-$, respectively.[15,16] The small oxidation peak at ≈−1.15 V_{Ag} has been assigned to $2S_4^{2-} \rightarrow S_8^{2-} + 2\ e^-$ (whereby $2S_4^{2-}$ can be produced via $S_8^{4-} \rightarrow 2S_4^{2-}$, see reaction 4).[15,16] This assignment is consistent with the fact that the small oxidation peak only appears when the reduction potential passes below the second reduction wave (i.e., after forming S_8^{4-}, see Figure S1a in the Supporting Information). The CV in DOL:DME (see red line in Figure 1) is noticeably distinct from that of DMSO and is consistent with the CV reported for pure DME.[16] The first electrochemical reduction step in DOL:DME occurs at a similar potential compared to DMSO if referred to the Ag/Ag^+ scale (Figure 1a), but as was observed previously,[16]

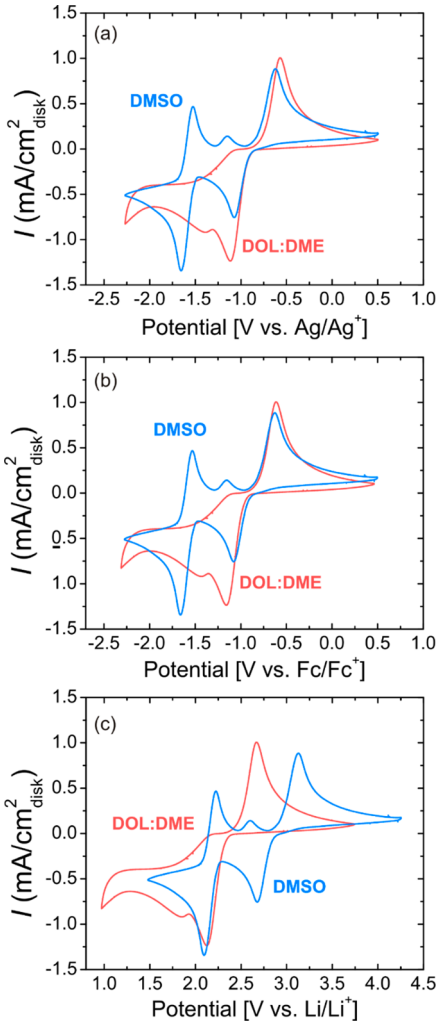

Figure 1. CVs of a GC electrode in 4 mM S_8−0.2 M $LiClO_4$ DMSO and 4 mM S_8−1.0 M LiTFSI DOL:DME (1:1) at 50 mV/s. (a) Potential versus Ag/Ag^+. (b) Potential versus Fc/Fc^+ (0 $mV_{Fc} \equiv -6$ mV_{Ag} for DMSO and 0 $mV_{Fe} \equiv -43$ mV_{Ag} for DOL:DME). (c) Potential versus Li/Li^+ (0 $V_{Li} \equiv -3.756$ $V_{Fc} \equiv -3.750$ V_{Ag} in DMSO and 0 $V_{Li} \equiv -3.283$ $V_{Fc} \equiv -3.240$ V_{Ag} in DOL:DME).

the separation between the first and the second reduction peaks nearly vanishes and the first oxidation peak during scan reversal (commencing at ≈−1.7 V_{Ag} in DMSO) cannot be observed anymore; oxidation only initiates at ≈−0.9 V_{Ag}, i.e., at the same potential where the second oxidation peak occurs in DMSO. The disappearance of the first oxidation peak is also observed in other low-dielectric solvents such as DME[16] and ionic liquids.[17] This possibly suggests a much reduced lifetime of the S_8^{4-} anion in DOL:DME compared to DMSO, but certainly reflects large differences in polysulfide solution chemistry between these solvents.

A more quantitative comparison of the potential dependence of the sulfur oxidation/reduction processes between the two electrolytes requires a reference potential scale for which possible junction potential differences between the working electrode and the Ag/Ag^+ reference electrode (a Ag wire immersed in ACN with 0.1 M $AgNO_3$ and separated by a Vycor frit from the working electrode compartment) are eliminated. This can be accomplished by referencing the working electrode potential to the redox potential of ferrocene added into the electrolyte in the working electrode compartment.[37] Following

dx.doi.org/10.1021/jp500382s | J. Phys. Chem. C 2014, 118, 5733−5741

this calibration (see Figure S2 in the Supporting Information), the Ag/Ag^+ reference scale in Figure 1a was converted into the ferrocene reference scale (indicated as V_{Fc}) shown in Figure 1b (note: 0 mV_{Fc} ≡ +6 mV_{Ag} for DMSO and 0 mV_{Fe} ≡ +43 mV_{Ag} for DOL:DME). Since the junction potentials are apparently very similar, the onset potentials of the first reduction peak and of the last oxidation peak are again very similar, indicating that at least the initial and the final sulfur reduction/oxidation potentials are comparable in both electrolytes. At first glance, this seems inconsistent with the substantial differences in charge/discharge plateaus which have been reported for lithium−sulfur battery cells using different electrolytes.[36,38]

However, rigorous comparison between CV data referred to a Ag/Ag^+ or a ferrocene reference electrode with charge/discharge data from battery cells requires that the CV data be referenced to the Li/Li^+ reference scale. This was accomplished by calibration of the ferrocene redox potential against a lithium metal strip in the working electrolyte. Surprisingly, the absolute difference between the Li/Li^+ potential and the ferrocene potential between DMSO and DOL:DME is very large, amounting to a potential difference of 0.432 V (0 V_{Li} ≡ −3.756 V_{Fc} ≡ −3.750 V_{Ag} in DMSO and 0 V_{Li} ≡ −3.283 V_{Fc} ≡ −3.240 V_{Ag} in DOL:DME). Thus, plotting the CVs against the Li/Li^+ reference scale in Figure 1c, the reduction of sulfur in DMSO seems to start at a ≈0.4 V higher potential than in DOL:DME, which now is consistent with the reported[28] strong solvent effect on charge/discharge potential in lithium−sulfur batteries. From the above discussion, however, it is clear that this is not caused by a significant difference in the onset potentials for sulfur reduction in these two electrolytes, but is caused by the substantially different Li/Li^+ redox potentials. In retrospect, this can easily be explained by Li^+ solvation energy differences in the two electrolytes, which can be inferred from the donor numbers of the solvents:[39] a rough estimate of the difference in Li^+-solvation energy between DMSO and DOL:DME (1:1) based on their donor numbers given in units of kcal/mol (DMSO ≈ 29.8,[40] DOL ≈ 18,[41] and DME ≈ 24[40]) yields a solvation energy difference of 36.8 kJ/mol (from 4.18 kJ/kcal × (29.8 − 0.5(18 + 24)). The estimated 36.8 kJ/mol higher Li^+ solvation energy in DMSO vs DOL:DME compares quite favorably to the observed 0.432 V lower Li/Li^+ potential in DMSO, equating to a solvation energy difference of 41.7 kJ/mol for a one-electron reaction.

A RRDE Approach To Probe Sulfur-Reduction/Oxidation. To gain more insight into the reaction mechanism and the physical origins responsible for the distinct CV responses observed in DMSO and DOL:DME, we performed RRDE measurements. Consistent with the CVs, the onset of sulfur reduction occurs at similar potential (vs V_{Fc}), but while two distinct diffusion limited current plateaus are observed for DMSO (blue lines in Figures 2b and 2c), only one current plateau is observed in DOL:DME (red lines in Figures 2b and 2c). The RRDE results referencing to the Ag/Ag^+ and Li/Li^+ scale are included in the Supporting Information (Figure S3). In principle, the number of electrons (n) transferred in each step can be determined from Levich−Koutecky plots of $1/i_L$ vs $\omega^{-1/2}$ (ω being the RRDE rotation rate), as shown in Figure S4 in the Supporting Information, if the sulfur concentration (c_{S8}), the electrolyte viscosity (ν), and the sulfur diffusion coefficient (D_{S8}) are known. Since c_{S8} is well-defined and since the viscosity can be easily quantified (see Supporting Information), the only value which must be obtained is D_{S8}. It was determined by stepping the disk potential from positive of

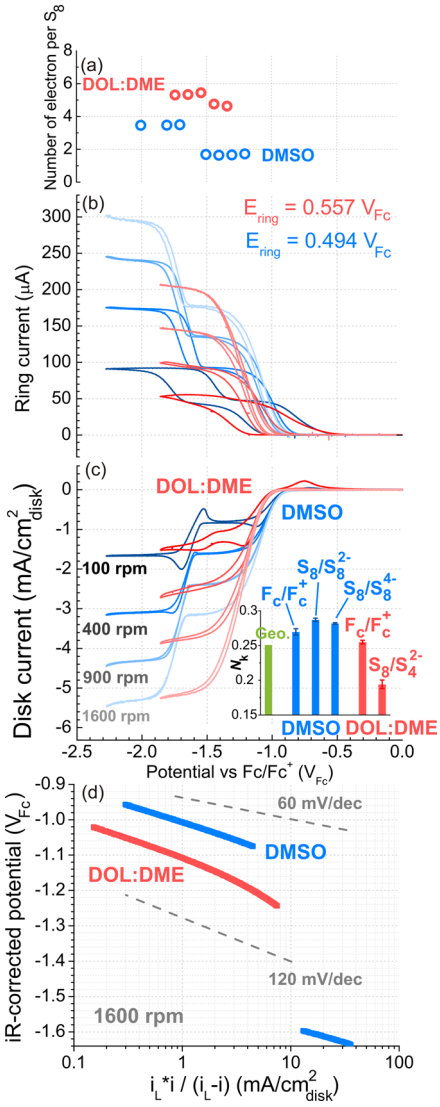

Figure 2. (a) Number of electrons transferred during the S reduction in DMSO and DOL:DME obtained using Levich−Koutecky slopes (Supporting Information Figure S4); diffusion coefficient of S_8 and viscosity of respective electrolytes are obtained experimentally (Figure S5 and Table S1 in the Supporting Information). Capacitively, non-ohmically corrected ring (b) and disk (c) currents recorded at 50 mV/s in Ar-saturated 4 mM S_8−0.2 M $LiClO_4$ DMSO (blue) and 4 mM S_8−1.0 M LiTFSI DOL:DME (1:1) (red) at rotation rates between 100 and 1600 rpm and continuously holding the Au ring electrode at 0.494 V_{Fc} for DMSO and at 0.557 V_{Fc} for DOL:DME. Inset: Calculated geometric collection efficiency (0.251) and the average collection efficiency of sulfur reaction observed in DMSO (first (S_8/S_8^{2-}), second (S_8/S_8^{2-}) waves, and the Fc/Fc^+ reference, see blue columns) and DOL:DME (S_8/S_4^{2-}) waves, and the Fc/Fc^+ reference, see red columns. (d) Kinetic currents measured in DMSO and DOL:DME. 60 mV/decade and 120 mV/decade lines are provided as a guide-to-the-eye for comparison. Note that 0 V_{Fc} ≡ +3.756 V_{Li} in DMSO and 0 V_{Fc} ≡ +3.283 V_{Li} in DOL:DME.

the sulfur reduction wave into the sulfur reduction potential, while holding the ring current at a negative potential where sulfur is being reduced continuously.

From the time delay (T_s) between stepping the disk potential and observing a change in the ring current (caused by a reduced sulfur flux to the ring electrode as sulfur is being consumed at the disk), the sulfur diffusion coefficient can be obtained via T_s

dx.doi.org/10.1021/jp500382s | J. Phys. Chem. C 2014, 118, 5733−5741

$= K(\upsilon/D)^{1/3}\omega^{-1}$, where K is a proportionality constant $K = 10.1$ rpm-s (for a detailed description see ref 32, Figure S5 in the Supporting Information, and the Supporting Information). Using these experimental D_{S8} values of 6.5×10^{-6} cm^2/s in DMSO with 0.2 M $LiClO_4$ (in good agreement with the reported 5.3×10^{-6} cm^2/s in DMSO with 0.1 M TEAP)[13] and of 2.6×10^{-6} cm^2/s in DOL:DME with 1 M LiTFSI, the number of electrons exchanged during the reaction can be determined (see Figure S4 and Table S1 in the Supporting Information) and is shown in Figure 2a.

Sulfur Reduction in DMSO. Based on this analysis, we can now examine the sulfur reduction processes for DMSO (blue lines/symbols in Figure 2). The first reduction wave (≈−0.9 to ≈−1.5 V_{Fc} corresponds to a 2-electron reduction (Figure 2a) of S_8 to S_8^{2-} according to reaction 1 and has a Tafel slope of ≈90 mV/decade (see the mass-transport and *iR*-loss corrected current density vs potential shown in Figure 2d), which would imply a transfer coefficient of $\alpha \approx 0.3$. The subsequent reduction wave at <−1.5 V_{Fc}) corresponds to a 4-electron reduction, which could be either a direct process (i.e., $S_8 + 4\ e^- \rightarrow S_8^{4-}$) or two 2-electron processes (i.e., $S_8 + 2\ e^- \rightarrow S_8^{2-}$ followed by $S_8^{2-} + 2\ e^- \rightarrow S_8^{4-} \rightarrow 2\ S_4^{2-}$). Considering the similar Tafel slope observed for the first and second reduction waves (i.e., similar rate-determining step in wave 1 and wave 2), we hypothesize that the second reduction wave is likely the series of two 2-electron processes with the second step being rate limiting. During these RRDE experiments, the ring electrode was held at a potential where all reduced sulfur species can be fully reoxidized to S_8, i.e., near the positive potential limit of +0.5 V_{Fc} used in the CVs (see Figure 1b). As one would expect, the ring/disk current ratio during the sulfur reduction on the disk electrode is close to the collection efficiency (N_k) of the RRDE (either calculated (denoted Geo.) or obtained by calibration with ferrocene; see inset in Figure 2c), indicating that all reduction species are dissolved in the electrolyte and can be mostly reoxidized on the ring in DMSO. During the RRDE measurement in DMSO, we observed the formation and accumulation of blue species in the solution, which has been attributed to the presence of $S_3^{\bullet-}$ by many other reports[5,11,14,15,19] and the formation of which is described by reactions 2 and 3. Interestingly, the CV responses showed no changes after the appearance of the blue species ($S_3^{\bullet-}$), suggesting that $S_3^{\bullet-}$ is not electrochemically active in the potential range used here.

Sulfur Reduction in DOL:DME. Contrary to the 2- and 4-electron transitions in DMSO, only one reduction step corresponding to ≈5 e^-/S_8 is observed in DOL:DME (red lines/symbols in Figure 2). One hypothesis to explain the drastic differences in the S reduction observed in DMSO and DOL:DME is the difference in the solvent's ability to solvate polysulfide anions. In general,[42] solvents with high dielectric constant such as DMSO (46.5[40]) exhibit stronger ability to stabilize charged species compared to solvents with low dielectric constant such as DME (7.075[40]) and DOL (7.13[40]). This is manifested by the formation of $S_3^{\bullet-}$ formed in DMSO[14] (and other high-dielectric solvents, see Figure S6 in the Supporting Information)[19,20] but not in DOL:DME (and other low-dielectric solvents, see Figure S6 in the Supporting Information, no blue coloration was observed during the CV and RRDE experiments in DOL:DME, in contrast to what was observed for DMSO). Our observation is consistent with a report by Manan et al.,[17] showing that $S_3^{\bullet-}$ is not formed in imidazolium ionic liquid even during extended bulk electrolysis and clear $S_3^{\bullet-}$ formation observed in DMSO. The range of dielectric constants for ionic liquids (including imidazolium) is between 10 and 15,[43] which is closer to DOL:DME than to DMSO. It is also consistent with a report by Tobishima et al.,[19] suggesting that the stability of polysulfide intermediates increases with the dielectric constant of the solvents. Thus, the two well-separated reduction waves observed in DMSO can be rationalized by strongly solvated and thus energetically stabilized S_8^{2-} anions so that their further electrochemical reduction requires a significantly more cathodic potential (≈0.6 V based on Figure 1b). On the contrary, if S_8^{2-} is weakly solvated and its formation is thus energetically unfavorable, its formation might be delayed until more cathodic potentials are reached, at which point multiple electron transfer reactions might occur. To probe the relationship between electrolyte solvation ability and S-reduction behavior, we replaced the weakly solvating cation, Li^+, with a strongly solvating cation, tetrabutylammonium TBA^+, in DOL:DME and performed RRDE measurements, as shown in Figure S7 in the Supporting Information. Remarkably, the "one" apparent S-reduction wave observed in LiTFSI DOL:DME changes into two distinct reduction waves in TBATFSI DOL:DME, which supports our hypothesis that the differences in the Li-RRDE results between DMSO (two waves) and DOL:DME (one wave) is related to the solvation ability of the solvent.

The reduction potential in DOL:DME is indeed ≈100 mV lower than in DMSO, as shown in Figure 2d. Furthermore, if correcting for the 5-fold higher Li^+ concentration in the DOL:DME electrolyte (corresponding to an ≈40 mV additional Nernstian shift in the redox potential for the reaction xLi + $x\ e^- + S_8 \rightarrow Li_xS_8$), the difference amounts to ≈140 mV.

The reaction sequence which leads to the apparent ≈5 e^-/S_8 reduction step in DOL:DME (see Figure 2a) is however not yet clear and may be understood by a more detailed analysis of the RRDE data. Here it is noteworthy that the ring/disk current ratio is significantly lower than the ferrocene-calibrated collection efficiency in DOL:DME (see inset in Figure 2c), which suggests that the reduction products in DOL:DME either cannot be reoxidized or do not reach the ring electrode. Since the ring potential is set to the positive potential limit used in the CVs (red line in Figure 1) and since the CVs are stable over many cycles, the formation of reduction products which cannot be reoxidized at the ring potential of +0.6 V_{Fc} (+3.84 V_{Li}!) is very unlikely. A more likely explanation may be the formation of solid reaction products on the disk electrode which would not be able to reach the ring electrode for reoxidation, thus leading to a lower ring/disk current ratio. Considering the poor solvation of polysulfides in DOL:DME, the reduced sulfur species might "break" or disproportionate in a way such that the number of charged and solvated polysulfides is minimized. Thus, one might imagine the following reaction:

$$4\ e^- + S_8 \rightarrow S_8^{4-} \rightarrow \downarrow S_1^{2-} + S_4^{2-} + (3/8)S_8 \qquad (7)$$

corresponding to a (2 + 2)-electron reduction followed by the cleavage of the S_8^{4-} at the two ends. The thus formed neutral sulfur could then get further reduced to S_4^{2-} according to

$$(3/2)e^- + (3/8)S_8 \rightarrow S_8^{4-} \rightarrow (3/4)S_4^{2-} \qquad (8)$$

The overall apparent number of electrons per S_8 would then be 5.5 e^-/S_8, and assuming that only the S_4^{2-} species could be reoxidized at the ring (the S_1^{2-} species precipitating on the disk

dx.doi.org/10.1021/jp500382s | J. Phys. Chem. C 2014, 118, 5733−5741

as Li_2S), the apparent ring/disk current ratio would be 64% of the collection efficiency, which is not too different from the observed 70%. Reactions 7 and 8 only served to outline one of many possibilities to obtain an apparent number of electrons which is higher than 4 e^-/S_8 without directly transferring more than 4 electrons in one step and to obtain at the same time a ring/disk current ratio which is less than the full collection efficiency. It, however, illustrates our hypothesis that low-dielectric solvents which are poor in stabilizing polysulfide anions might favor the formation and precipitation of insoluble sulfides like Li_2S.

Bridging RRDE and Lithium–Sulfur Batteries: A Lithium–Sulfur Catholyte Cell Approach. Considering the fact that the total numbers of electrons involved during the Li-RRDE measurements in DMSO (4 e^-/S_8) and DOL:DME (≈5 e^-/S_8) are only about one-quarter of the total expected charge for the complete reduction of S_8 (16 e^-/S_8), we hypothesize that only part of the total discharge capacity in the Li–S batteries is obtained through direct *electrochemical steps*, and that the rest of the capacity must be achieved via various subsequent chain-growth and disproportionation reactions that generate sulfur (S_8) or reducible polysulfides (e.g., S_8^{2-}). If our above hypothesis that the instability of polysulfides in low-dielectric solvent favors the precipitation of insoluble sulfides (i.e, Li_2S) were true, one would thus expect a higher rate capability for DOL:DME compared to DMSO. However, to test this hypothesis, the reaction of polysulfides at the anode (shuttling effect) must be avoided and the sulfur in the cathode must be 100% accessible. This is accomplished by the here used battery cell design, where a lithium ion conducting and otherwise impermeable membrane (lithium ion conducting solid electrolyte) is located in between anode and cathode compartment and where the sulfur is completely dissolved in the catholyte and held within a carbon fiber paper with a total carbon surface area of 18 cm^2_C (see Supporting Information; the basic cell design is given in refs 35 and 44). The amount of sulfur in the catholyte is 2.05 × 10^{-5} g_s, so that the applied current range of 2–100 μA in galvanostatic charge/discharge curves corresponds to rates of C/17 to 3 C (based on 1672 $mA/g_s \equiv 1$ C); if full conversion to Li_2S were achieved, 123 mC of charge would be obtained.

Lithium–Sulfur Catholyte Cell Using DMSO. The galvanostatic discharge/charge curves at different currents in DMSO with 0.2 M $LiClO_4$ are shown in Figure 3a, showing a first and a second discharge plateau, which is consistent with those observed in RDE measurements (Figure S3 in the Supporting Information shows the RRDE data vs the Li/Li^+ reference scale). It is noteworthy that, at a very slow rate (2 μA ≡ C/17), all of the sulfur can be converted to Li_2S, corresponding to the full 16 e^-/S_8; the much lower 4 e^-/S_8 which were obtained in RRDE experiments (time scale of seconds) are due to the ≈10^4-fold longer reaction time in the battery cell. Considering that the highest reversible capacity reported for Li–S cells in the literature is about 75% of the theoretical capacity,[23,24] as pointed out recently by Cuisinier et al.,[29] we believe that the reason we could obtain 100% theoretical capacity in the Li–S catholyte cell is due to the facts that (1) the lithium ion conducting solid electrolyte eliminates the loss of active material (i.e., sulfur and polysulfides) to the anode side and (2) the sulfur is fully dissolved in the electrolyte, which provides 100% sulfur accessibility. With increasing discharge currents, the capacity decreases rapidly, whereby only the capacity in the lower voltage plateau diminishes while

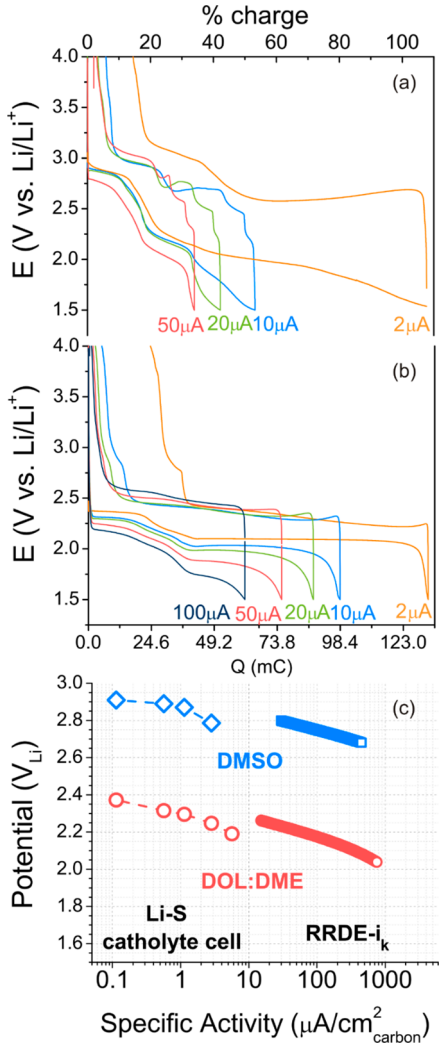

Figure 3. Galvanostatic discharge and charge profiles of Li–S catholyte cell consist of (a) Li/0.2 M $LiClO_4$ DMSO/glass fiber/Ohara glass/carbon paper–20 μL of 4 mM S_8–0.2 M $LiClO_4$ DMSO and (b) Li/1.0 M LiTFSI DOL:DME (1:1)/glass fiber/Ohara glass/carbon paper–20 μL of 4 mM S_8–1.0 M LiTFSI DOL:DME (1:1). Operation rate range from 2 μA (≡C/17) to 100 μA (≡3C). (c) Specific activity of S reduction obtained via Li–S catholyte cell and RRDE kinetic current (i_k). The roughness factor of carbon paper and glassy carbon is estimated to be 10 $cm^2_{carbon}/cm^2_{disk}$.

that of the higher voltage plateau remains essentially constant, comprising about 20% of the theoretical capacity (counting from the high-voltage plateau until the beginning of the low-voltage plateau). This value corresponds very closely to the 2.7 e^-/S_8 (≈17% of the theoretical capacity) which would be obtained from reactions 1 and 2 ($(3/4)S_8 + 2\ e^- \rightarrow S_6^{2-}$). This implies that the initial electrochemical reduction is very fast compared to the solution-phase chain-growth/disproportionation which is required to achieve the full reduction to Li_2S.

At the highest current of 50 μA (≡1.5 C) only about 1/3 of the theoretical capacity is reached, which is only slightly above the value which could be obtained by purely electrochemical reduction of sulfur (i.e., 4 e^-/S_8 ≡ 25% theoretical capacity) and which is quite poor compared to what can be achieved in current lithium–sulfur batteries.[3,4,25,45–47] Nevertheless, the RRDE and cell data agree very well, which is also demonstrated by the fact that the specific currents in the upper discharge

dx.doi.org/10.1021/jp500382s | J. Phys. Chem. C 2014, 118, 5733–5741

Scheme 1. Proposed Sulfur Reduction Reaction Mechanism

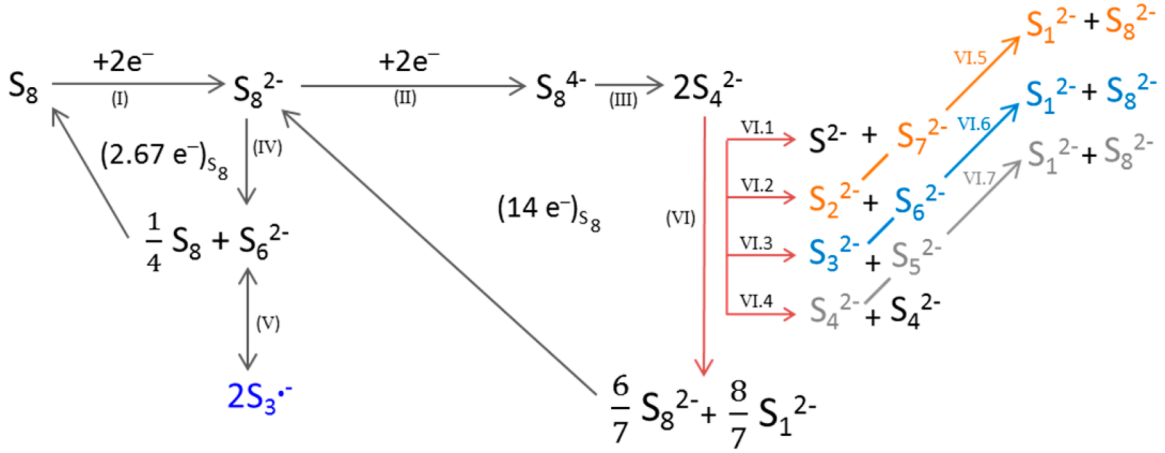

plateau shown in Figure 3a are reasonably consistent with what one would expect based on the kinetic currents measured in the RRDE (see Figure 3c).

Lithium−Sulfur Catholyte Cell Using DOL:DME. Similar to the above data in DMSO, the upper voltage plateau of the cell with 1 M LiTFSI in DOL:DME (see Figure 3b) is consistent with the onset voltage in the RRDE data (see Figure S3 in the Supporting Information), and 100% capacity (16 e^-/S_8) is obtained at 2 μA (≡C/17). Also, the capacity of the first voltage plateau of ≈30% (counting up to the beginning of the second plateau) is consistent with the ≈5 e^-/S_8 (≡31%) obtained in the RRDE experiments, and essentially no rate dependence is observed. Again, this is related to the fast kinetics of the electrochemical steps, which are comparable to those measured in the RRDE (see Figure 3c). However, in contrast to the cell data with DMSO, the rate capability in the lower voltage plateau is significantly higher, yielding 60% capacity at 50 μA (≡1.5 C) compared to 30% with DMSO. Furthermore, the voltage hysteresis between charge and discharge is much smaller in the case of DOL:DME. This strongly supports our above hypothesis that the poor stabilization of polysulfides in low-dielectric solvents favors the formation of solid precipitates (i.e., forming $Li_2S_{(s)}$ on the discharge and forming $S_{8(s)}$ on the charge) and thus leads to a higher rate capability in the lower voltage plateau where rates are controlled by polysulfide chain-growth/disproportionation.

We summarize the S-reduction mechanism in Scheme 1. The elemental sulfur is first reduced via a 2-electron process to form S_8^{2-} (reaction I), which is followed by a 2-electron process to form S_8^{4-} (reaction II) with a subsequent dissociation forming $2S_4^{2-}$ (reaction III) or by a disproportionation reaction to form (1/4)S_8 and S_6^{2-} (reaction IV), which dissociates to $S_3^{\bullet-}$ (blue species, reaction V). The sulfur formed in reaction IV can be further reduced, leading to an overall 2.67 e^-/S_8 process. Reactions I, II, and III occur in both DMSO and DOL:DME while reactions IV and V occur only in DMSO, as evidenced by the formation of $S_3^{\bullet-}$ (blue species) in DMSO-RRDE measurements and the first discharge plateau having approximately 20% capacity (i.e., close to 2.7 e^-/S_8) in the DMSO−Li−S catholyte cell (Figure 3a). This is explained by that the polysulfide radical $S_3^{\bullet-}$ is better stabilized by high-dielectric solvent such as DMSO compared to the low-dielectric solvent such as DOL:DME. To achieve full capacity (16 e^-/S_8) without involving electrochemical steps beyond 4 e^-/S_8, we hypothesize that the S_4^{2-} polysulfide anions undergo various subsequent chain-growth and disproportionation reactions to generate reducible species such as S_8, S_8^{2-}. One example is illustrated in reaction VI (see Scheme 1): two S_4^{2-} anions could combine and dissociate to S_n^{2-} and $S_{(8-n)}^{2-}$, n = 1, 2, 3, 4 (reactions VI.1−VI.4) followed by a combination between S_n^{2-} and $S_{(9-n)}^{2-}$, n = 2, 3, 4 to give S_1^{2-} and S_8^{2-} (reactions VI.5−VI.7). Such a scenario is equivalent to the formation of ((8/7)S_1^{2-} + (6/7)S_8^{2-}) from $2S_4^{2-}$ (reaction VI). The further electrochemical reduction of (6/7)S_8^{2-} via the same route (i.e., reactions II → III → VI) will lead to a total 14 e^-/S_8 process (see Scheme 1).

CONCLUSION

Our study shed light on the sulfur reduction mechanism and highlights the strong influence of solvent's solvation power on rate capability of Li−S batteries. We exploited rotating RRDE voltammetry and the specially designed Li−sulfur catholyte cells to examine sulfur charge/discharge behavior in low- vs high-dielectric solvents (i.e., DOL:DME vs DMSO). We show that only part of the sulfur reduction capacity is obtained through direct *electrochemical steps*, and that the rest of the capacity is achieved via various subsequent chain-growth and disproportionation reactions that generate reducible species. The rates of these chain-growth/disproportionation reactions are higher in low-dielectric solvents such as DOL:DME compared to high-dielectric solvents such as DMSO due to its poor stabilization of polysulfides, which leads to a higher rate capability in the Li−S batteries.

ASSOCIATED CONTENT

Supporting Information

Experimental details about chemicals, rotating-ring disk electrode measurement, measurements of diffusion coefficient of polysulfide, CV and RRDE results with respect to silver (Ag/Ag^+) and lithium (Li/Li^+), junction potential calibration, Levich−Koutecky plots, transient time, images of chemically made "Li_2S_8" in various solvents, and RRDE results in 4 mM S_8−1.0 M TBATFSI DOL:DME. This material is available free of charge via the Internet at http://pubs.acs.org.

AUTHOR INFORMATION

Corresponding Author

*E-mail: yichunlu@mae.cuhk.edu.hk. Mailing address: Mechanical and Automation Engineering, Room 214, William M.W.

dx.doi.org/10.1021/jp500382s | J. Phys. Chem. C 2014, 118, 5733−5741

Mong Engineering Building, Chinese University of Hong Kong, Shatin, N.T., Hong Kong SAR, China. Tel: +852-3943-8339.

Notes

The authors declare no competing financial interest.

■ ACKNOWLEDGMENTS

The authors are grateful to Dr. Juan Herranz-Salaner and Armin Siebel for RRDE cell design and scientific discussion, Dr. Himendra Jha for experimental assistance and scientific discussion, and Johannes Hattendorff for the measurement of solvent viscosity. We are grateful for financial support of this research by the Bavarian Ministry of Economic Affairs and Media, Energy and Technology performed under the auspices of the EEBatt project.

■ REFERENCES

(1) Bruce, P. G.; Freunberger, S. A.; Hardwick, L. J.; Tarascon, J. M. Li-O_2 and Li-S Batteries With High Energy Storage. *Nat. Mater.* **2012**, *11*, 19−29.

(2) Ellis, B. L.; Lee, K. T.; Nazar, L. F. Positive Electrode Materials for Li-Ion and Li-Batteries. *Chem. Mater.* **2010**, *22*, 691−714.

(3) Ji, X.; Nazar, L. F. Advances in Li-S Batteries. *J. Mater. Chem.* **2010**, *20*, 9821−9826.

(4) Yin, Y.-X.; Xin, S.; Guo, Y.-G.; Wan, L.-J. Lithium−Sulfur Batteries: Electrochemistry, Materials, and Prospects. *Angew. Chem., Int. Ed.* **2013**, *52*, 13186−13200.

(5) Fujinaga, T.; Kuwamoto, T.; Okazaki, S.; Hojo, M. Electrochemical Reduction of Elemental Sulfur in Acetonitrile. *Bull. Chem. Soc. Jpn.* **1980**, *53*, 2851−2855.

(6) Evans, A.; Montenegro, M. I.; Pletcher, D. The Mechanism for the Cathodic Reduction of Sulphur in Dimethylformamide: Low Temperature Voltammetry. *Electrochem. Commun.* **2001**, *3*, 514−518.

(7) Han, D.-H.; Kim, B.-S.; Choi, S.-J.; Jung, Y.; Kwak, J.; Park, S.-M. Time-Resolved In Situ Spectroelectrochemical Study on Reduction of Sulfur in N,N-Dimethylformamide. *J. Electrochem. Soc.* **2004**, *151*, E283−E290.

(8) Leghié, P.; Lelieur, J. P.; Levillain, E. Comments on the Mechanism of the Electrochemical Reduction of Sulphur in Dimethylformamide. *Electrochem. Commun.* **2002**, *4*, 406−411.

(9) Leghié, P.; Lelieur, J. P.; Levillain, E. Final Comment on Reply to "Comments On the Mechanism of the Electrochemical Reduction of Sulphur in Dimethylformamide. *Electrochem. Commun.* **2002**, *4*, 628.

(10) Levillain, E.; Gaillard, F.; Leghie, P.; Demortier, A.; Lelieur, J. P. On the Understanding of the Reduction of sulfur (S_8) in Dimethylformamide (DMF). *J. Electroanal. Chem.* **1997**, *420*, 167−177.

(11) Badoz-Lambling, J.; Bonnaterre, R.; Cauquis, G.; Delamar, M.; Demange, G. La Reduction du Soufre en Milieu Organique. *Electrochim. Acta* **1976**, *21*, 119−131.

(12) Kim, B. S.; Park, S. M. In Situ Spectroelectrochemical Studies on the Reduction of Sulfur in Dimethyl Sulfoxide Solutions. *J. Electrochem. Soc.* **1993**, *140*, 115−122.

(13) Baranski, A. S.; Fawcett, W. R.; Gilbert, C. M. Use of Microelectrodes for the Rapid Determination of the Number of Electrons Involved in an Electrode Reaction. *Anal. Chem.* **1985**, *57*, 166−170.

(14) Bonnaterre, R.; Cauquis, G. Spectrophotometric Study of the Electrochemical Reduction of Sulphur in Organic Media. *J. Chem. Soc., Chem. Commun.* **1972**, 293−294.

(15) Martin, R. P.; Doub, W. H.; Roberts, J. L.; Sawyer, D. T. Electrochemical Reduction of Sulfur in Aprotic Solvents. *Inorg. Chem.* **1973**, *12*, 1921−1925.

(16) Jung, Y.; Kim, S.; Kim, B. S.; Han, D. H.; Park, S. M.; Kwak, J. Effect of Organic Solvents and Electrode Materials on Electrochemical Reduction of Sulfur. *Int. J. Electrochem. Sci.* **2008**, *3*, 566−577.

(17) Manan, N. S. A.; Aldous, L.; Alias, Y.; Murray, P.; Yellowlees, L. J.; Lagunas, M. C.; Hardacre, C. Electrochemistry of Sulfur and Polysulfides in Ionic Liquids. *J. Phys. Chem. B* **2011**, *115*, 13873−13879.

(18) Chivers, T.; Drummond, I. Characterization of Trisulfur Radical Anion S^{3-} in Blue Solutions of Alkali Polysulfides in Hexamethylphosphoramide. *Inorg. Chem.* **1972**, *11*, 2525−2525.

(19) Tobishima, S. I.; Yamamoto, H.; Matsuda, M. Study on the Reduction Species of Sulfur by Alkali Metals in Nonaqueous Solvents. *Electrochim. Acta* **1997**, *42*, 1019−1029.

(20) Rauh, R. D.; Shuker, F. S.; Marston, J. M.; Brummer, S. B. Formation of Lithium Polysulfides in Aprotic Media. *J. Inorg. Nucl. Chem.* **1977**, *39*, 1761−1766.

(21) Gaillard, F.; Levillain, E.; Lelieur, J. P. Polysulfides in Dimethylformamide: Only the Radical Anions S^{3-} and S^{4-} are Reducible. *J. Electroanal. Chem.* **1997**, *432*, 129−138.

(22) Levillain, E.; Gaillard, F.; Lelieur, J. P. Polysulfides in Dimethylformamide: Only the Redox Couples S^{-n}/S^{2-n} are Involved. *J. Electroanal. Chem.* **1997**, *440*, 243−250.

(23) Akridge, J. R.; Mikhaylik, Y. V.; White, N. Li/S Fundamental Chemistry and Application to High-Performance Rechargeable Batteries. *Solid State Ionics* **2004**, *175*, 243−245.

(24) Elazari, R.; Salitra, G.; Garsuch, A.; Panchenko, A.; Aurbach, D. Sulfur-Impregnated Activated Carbon Fiber Cloth as a Binder-Free Cathode for Rechargeable Li-S Batteries. *Adv. Mater.* **2011**, *23*, 5641−5644.

(25) Barchasz, C.; Molton, F.; Duboc, C.; Leprêtre, J.-C.; Patoux, S.; Alloin, F. Lithium/Sulfur Cell Discharge Mechanism: An Original Approach for Intermediate Species Identification. *Anal. Chem.* **2012**, *84*, 3973−3980.

(26) Walus, S.; Barchasz, C.; Colin, J.-F.; Martin, J.-F.; Elkaim, E.; Lepretre, J.-C.; Alloin, F. New Insight into the Working Mechanism of Lithium-Sulfur Batteries: In Situ and Operando X-ray Diffraction Characterization. *Chem. Commun.* **2013**, *49*, 7899−7901.

(27) Barchasz, C.; Leprêtre, J.-C.; Patoux, S.; Alloin, F. Electrochemical Properties of Ether-Based Electrolytes for Lithium/Sulfur Rechargeable Batteries. *Electrochim. Acta* **2013**, *89*, 737−743.

(28) Gao, J.; Lowe, M. A.; Kiya, Y.; Abruña, H. D. Effects of Liquid Electrolytes on the Charge−Discharge Performance of Rechargeable Lithium/Sulfur Batteries: Electrochemical and In-Situ X-ray Absorption Spectroscopic Studies. *J. Phys. Chem. C* **2011**, *115*, 25132−25137.

(29) Cuisinier, M.; Cabelguen, P.-E.; Evers, S.; He, G.; Kolbeck, M.; Garsuch, A.; Bolin, T.; Balasubramanian, M.; Nazar, L. F. Sulfur Speciation in Li−S Batteries Determined by Operando X-ray Absorption Spectroscopy. *J. Phys. Chem. Lett.* **2013**, *4*, 3227−3232.

(30) Ueno, K.; Park, J.-W.; Yamazaki, A.; Mandai, T.; Tachikawa, N.; Dokko, K.; Watanabe, M. Anionic Effects on Solvate Ionic Liquid Electrolytes in Rechargeable Lithium−Sulfur Batteries. *J. Phys. Chem. C* **2013**, *117*, 20509−20516.

(31) Wang, L.; Byon, H. R. N-Methyl-N-propylpiperidinium bis(trifluoromethanesulfonyl)imide-Based Organic Electrolyte for High Performance Lithium−Sulfur Batteries. *J. Power Sources* **2013**, *236*, 207−214.

(32) Herranz, J.; Garsuch, A.; Gasteiger, H. A. Using Rotating Ring Disc Electrode Voltammetry to Quantify the Superoxide Radical Stability of Aprotic Li-Air Battery Electrolytes. *J. Phys. Chem. C* **2012**, *116*, 19084−19094.

(33) Trahan, M. J.; Mukerjee, S.; Plichta, E. J.; Hendrickson, M. A.; Abraham, K. M. Studies of Li-Air Cells Utilizing Dimethyl Sulfoxide-Based Electrolyte. *J. Electrochem. Soc.* **2013**, *160*, A259−A267.

(34) Mikhaylik, Y. V.; Akridge, J. R. Polysulfide Shuttle Study in the Li/S Battery System. *J. Electrochem. Soc.* **2004**, *151*, A1969−A1976.

(35) Rebecca, B.; Meini, S.; Gasteiger, H. A. On-Line Electrochemical Mass Spectrometry Investigations on the Gassing Behavior of $Li_4Ti_5O_{12}$ Electrodes and its Origins. *J. Electrochem. Soc.* **2014**, *161*, A497−A505.

(36) Kolosnitsyn, V. S.; Karaseva, E. V.; Seung, D. Y.; Cho, M. D. Cycling a Sulfur Electrode: Effect of Physicochemical Properties of Electrolyte Systems. *Russ. J. Electrochem.* **2003**, *39*, 1089−1093.

(37) Gritzner, G.; Kůta, J. Recommendations on Reporting Electrode Potentials in Nonaqueous Solvents. *Pure Appl. Chem.* **1984**, *56*, 461−466.
(38) Guo, J.; Yang, Z.; Yu, Y.; Abruña, H. D.; Archer, L. A. Lithium−Sulfur Battery Cathode Enabled by Lithium−Nitrile Interaction. *J. Am. Chem. Soc.* **2012**, *135*, 763−767.
(39) Gutmann, V. Empirical Parameters for Donor and Acceptor Properties of Solvents. *Electrochim. Acta* **1976**, *21*, 661−670.
(40) Aurbach, D.; Weissman, I. In *Nonaqueous Electrochemistry*; Aurbach, D., Ed.; CRC Press: Boca Raton, 1999.
(41) Jin, Z.; Xie, K.; Hong, X. Synthesis and Electrochemical Properties of a Perfluorinated Ionomer with Lithium Sulfonyl Dicyanomethide Functional Groups. *J. Mater. Chem. A* **2013**, *1*, 342−347.
(42) Carey, F.; Sundberg, R. In *Advanced Organic Chemistry*; Springer: New York, 2007; pp 253−388.
(43) Krossing, I.; Slattery, J. M.; Daguenet, C.; Dyson, P. J.; Oleinikova, A.; Weingärtner, H. Why Are Ionic Liquids Liquid? A Simple Explanation Based on Lattice and Solvation Energies. *J. Am. Chem. Soc.* **2006**, *128*, 13427−13434.
(44) Meini, S.; Piana, M.; Tsiouvaras, N.; Garsuch, A.; Gasteiger, H. A. The Effect of Water on the Discharge Capacity of a Non-Catalyzed Carbon Cathode for Li-O_2 Batteries. *Electrochem. Solid State Lett.* **2012**, *15*, A45−A48.
(45) Wang, D.; Yu, Y.; Zhou, W.; Chen, H.; DiSalvo, F. J.; Muller, D. A.; Abruna, H. D. Infiltrating Sulfur in Hierarchical Architecture MWCNT@meso C Core-Shell Nanocomposites for Lithium-Sulfur Batteries. *Phys. Chem. Chem. Phys.* **2013**, *15*, 9051−9057.
(46) Aurbach, D.; Pollak, E.; Elazari, R.; Salitra, G.; Kelley, C. S.; Affinito, J. On the Surface Chemical Aspects of Very High Energy Density, Rechargeable Li−Sulfur Batteries. *J. Electrochem. Soc.* **2009**, *156*, A694−A702.
(47) Ji, X.; Lee, K. T.; Nazar, L. F. A Highly Ordered Nanostructured Carbon-Sulphur Cathode for Lithium-Sulphur Batteries. *Nat. Mater.* **2009**, *8*, 500−506.